BG-20-839-2023

Temporal patterns of greenhouse gas emissions from two small thermokarst lakes in Nunavik, Canada

Responses to Anonymous Referee #2

We would like to thank the reviewer for their helpful contribution to the article. Please note that additions to the article are shown in **bold**. The lines in this document refer to the previous version of the manuscript and may be subject to change in the revised version.

1. General remarks

Here, Pouliot et al. conducted an intensive study on GHG emissions in two thermokarst lakes located within the same ecosystem but exhibiting contrasting limnological characteristics. The study primarily aims to synthesize data from two consecutive summer sampling campaigns, its main strength lies in the high-resolution diel and summer temporal sampling of GHG gases, as well several associated biophysical and environmental parameters. However, I recommend moderating the strong extrapolations made from these limited summer datasets to broader seasonal year dynamics. The study would be more robust if it is focused on summer observations and cautiously discussed the potential implications for winter and turnover periods before and after ice cover. I would argue that such extrapolation is quite vague, given that the diel patterns differ between the two sampling days across different years, even in subsequent day measurements in same ecosystem (Figure 5), data varies importantly. Therefore, your statement remains unclear whether these differences are due to actual environmental changes or simply the result of capturing a single day per year, which may not adequately represent diel or yearly variability. Below see other comments about the manuscript that would help you to improve it.

Thank you for this important comment. We agree that the seasonal estimates based on limnophysical indicators and bottom gas concentrations are subject to uncertainty due to the absence of direct year-round GHG flux measurements. In response, we have revised the study's objectives to clarify that the focus of the study is on understanding the drivers of summer temporal variations in GHG fluxes by measuring them, and emphasize the exploration of seasonal patterns using limnophysical proxies, rather than directly measuring seasonal GHG emissions. We also suggest moving the Methodology and corresponding Results sections on seasonal extrapolations, including Table 5, to the Supplementary Material. Consequently, these extrapolations would only be covered in the Discussion section, which we have also modified to improve clarity. Finally, we propose toning down the conclusions regarding seasonal patterns, presenting them now as hypothesis-generating interpretations rather than firm conclusions.

2. Major concerns

2.1. Please work on improving the methodology section as it is currently difficult to follow. Consider moving some detailed information to the appendix or supplementary materials, while expanding explanation of key topics. A comprehensive data table would help clarify your sampling approach. For example, it is unclear how many samples were collected for the diel analysis, subsequent days GHG measurements during the summer campaigns, and other parameters. I said this because, I cannot determine the source of

the N values reported in Tables 3 and 4 or whether they come from the diel sampling. Besides, consider consolidating related tables (e.g., Tables 1 and 2 could be merged).

Thank you for your helpful suggestions. Removing the "larger-scale estimates" section (see response to Comment 1) shortened the Methods section by approximately 23%, thereby improving its readability. Regarding the diel analysis, rather than collecting data continuously over a single 24-h period, we measured fluxes and gas concentrations at various times over multiple days. This enabled us to gradually reconstruct a full diel cycle. To clarify the sampling strategy, we propose adding the following to the Methodology:

> Line 201: To estimate GHG fluxes, we measured both dissolved gas concentrations (CO_2, CH_4, and N_2O) and CO_2 diffusive fluxes using a floating chamber **during the intensive summer campaigns in July 2022 and August 2023. At each lake, measurements were taken over multiple consecutive days across different hours of the day and night. This approach enabled us to reconstruct diel variability in gas fluxes, dissolved gas concentrations, and k_{600}, yielding between 9 and 13 data points per lake for both intensive campaigns.**

We also propose presenting the results more transparently and revising the titles of Figure 9 and 10 to improve clarity:

> Line 480: **Measurements of CO_2 fluxes, dissolved gas concentrations, and k_{600} over multiple consecutive days across different hours allowed us to reconstruct diel variability for both intensive campaigns (Fig. 9).** In 2022, no discernible diel patterns were observed in either the surface concentrations (Fig. S7a,b,c), the gas transfer coefficient (Fig. S8a), or the diffusive emissions of CO_2, CH_4, and N_2O (Fig. 9a,b,c).

> Figure 9. Diel cycles of CO_2 (a,d), CH_4 (b,e) and N_2O (c,f) diffusive fluxes for the July 2022 (left) and August 2023 (right) intensive summer campaign periods. CO_2 fluxes were measured directly with the floating chamber, while CH_4 and N_2O fluxes were obtained by applying the k values derived from CO_2 fluxes to their respective concentrations. The grey dotted line represents atmospheric equilibrium, and the grey shaded area indicates periods of zero solar radiation. **Although the data are presented on a diurnal cycle, the measurements were taken over a two-week period (see Table S2).** Coloured dotted lines represent sine-fitted trend lines. Time of day is expressed in EST.

To improve the traceability of the samplings, we propose adding Table S4, which will list all dissolved gas concentration measurements used in the study, and modifying Table S6 to include descriptive values for k_{600} rather than just mean, min and max values:

Table S4. Dissolved gases measurements at lakes TAS1 and TAS3 in July 2022 and August 2023. Time of day is expressed in EST.

	July 2022				August 2023			
Lake	Date	CO_2 (µM)	CH_4 (µM)	N_2O (µM)	Date	CO_2 (µM)	CH_4 (µM)	N_2O (µM)
TAS1	2022-07-06 14:20	36.30	2.26	0.015	2023-08-09 14:30	21.43	3.22	0.004
	2022-07-07 08:46	40.90	1.44	0.014	2023-08-10 11:50	34.07	3.13	0.004
	2022-07-07 13:24	35.48	1.36	0.015	2023-08-11 18:59	24.39	1.99	0.005
	2022-07-11 01:46	43.34	0.92	0.015	2023-08-12 22:10	28.80	1.07	0.005
	2022-07-11 16:44	29.01	0.97	0.013	2023-08-13 17:59	29.19	1.42	0.004
	2022-07-12 12:08	37.85	1.06	0.013	2023-08-14 10:12	46.01	1.28	0.004
	2022-07-12 19:08	26.96	1.06	0.013	2023-08-14 13:20	25.41	1.58	0.004
	2022-07-13 09:21	40.12	0.97	0.014	2023-08-15 00:40	44.05	1.20	0.004
	2022-07-13 10:45	36.48	1.28	0.014	2023-08-15 16:20	34.32	1.39	0.004
	2022-07-15 04:33	43.20	1.57	0.013	2023-08-16 04:30	71.83	1.86	0.003
					2023-08-18 11:00	100.14	1.41	0.003
					2023-08-19 7:20	122.48	2.37	0.004
					2023-08-20 7:20	81.95	1.29	0.004
TAS3	2022-07-06 15:27	28.10	0.47	0.015	2023-08-09 15:22	28.79	1.06	0.004
	2022-07-07 10:24	27.95	0.59	0.015	2023-08-11 19:59	51.36	3.43	0.003
	2022-07-07 14:08	24.08	0.44	0.013	2023-08-12 22:59	58.84	1.87	0.003
	2022-07-08 08:23	34.33	0.51	0.015	2023-08-13 19:27	30.13	1.94	0.004
	2022-07-11 00:24	27.53	0.45	0.014	2023-08-14 11:29	55.25	2.06	0.003
	2022-07-11 16:57	16.97	0.39	0.012	2023-08-14 14:22	30.57	1.82	0.003
	2022-07-12 11:26	23.41	0.37	0.013	2023-08-15 01:50	218.85	3.07	0.003
	2022-07-12 20:07	10.15	0.30	0.012	2023-08-15 17:30	28.54	2.84	0.003
	2022-07-13 08:30	32.28	0.43	0.012	2023-08-16 06:59	117.43	2.69	0.003
					2023-08-18 12:12	154.99	5.49	0.003
					2023-08-19 08:35	236.16	9.88	0.004
					2023-08-20 08:20	119.01	5.50	0.004

Table S6. Gas transfer velocities (k_{600}) measured with the floating chamber in lakes TAS1 and TAS3 using surface GHG concentrations obtained by the headspace method. Time of day is expressed in EST.

	July 2022		August 2023	
Lake	Date	k_{600} (cm h^{-1})	Date	k_{600} (cm h^{-1})
TAS1	2022-07-07 09:14	4.00	2023-08-10 11:50	10.12
	2022-07-07 13:36	4.18	2023-08-11 19:10	9.80
	2022-07-11 01:59	4.51	2023-08-12 22:41	3.19
	2022-07-11 16:09	4.97	2023-08-13 18:18	4.88
	2022-07-12 11:53	4.08	2023-08-14 10:28	5.76
	2022-07-12 19:03	2.54	2023-08-14 13:48	11.01
	2022-07-13 08:37	1.57	2023-08-15 01:23	1.61
	2022-07-13 10:51	4.29	2023-08-15 16:55	4.46
	2022-07-15 04:19	1.62	2023-08-16 05:09	4.37
			2023-08-18 11:41	4.13
			2023-08-19 08:00	3.09
			2023-08-20 08:00	5.36
TAS3	2022-07-07 10:41	2.89	2023-08-11 20:19	2.38
	2022-07-07 14:22	1.96	2023-08-12 23:36	1.60
	2022-07-08 08:42	1.78	2023-08-13 19:42	3.03
	2022-07-11 00:59	2.57	2023-08-14 11:45	4.52
	2022-07-12 11:11	1.17	2023-08-14 14:42	8.19
	2022-07-12 19:47	1.36	2023-08-15 02:15	0.45
	2022-07-13 09:50	1.48	2023-08-15 17:53	2.98
			2023-08-16 07:18	2.54
			2023-08-18 12:46	1.88
			2023-08-19 08:54	1.33
			2023-08-20 09:03	3.43

Regarding Tables 1 and 2, we prefer to keep them separate to maintain clarity on site-specific characteristics. However, Table 4 overlapped with information shown in Figure 7, and therefore we propose moving it to the Supplementary Material.

2.2. Regarding buoyancy frequency calculations, please clarify how you determined water density in the ponds. Did you incorporate your measurements or use arbitrary values? This section needs a more detailed explanation.

Thank you for this comment. Water density was calculated based on our in-situ measurements of temperature at surface and bottom of the lakes. We have now added this explanation to the methodology section:

Line 164: The buoyancy frequency (N, cycles per hour), which quantifies water column stability, was calculated using the following equation:

$$N = \sqrt{-\frac{g}{\rho}\frac{d\rho}{dz}}\frac{3600}{2\pi} \quad (1)$$

where g is the acceleration due to gravity (9.81 m s^{-2}), ρ is the water density (kg m^{-3}), and z is the depth (m). **We derived water density from our in situ temperature measurements at the surface and bottom of each lake using the Kell equation (Jones and Harris, 1992). This enabled us to estimate the vertical water density gradient ($d\rho/dz$).**

2.3. The CH_4 ebullition methodology requires expansion, particularly since it represented the primary CH_4 source to the atmosphere in one pond. Please explain the bubble trap attachment system that prevented movement during the 11-day deployment. Additionally, specify the number of bubble traps used and their spatial distribution across the lake. The issue arises because small replicate ebullition traps may not fully capture ebullition events, Wik et al. (2016, doi: 10.1002/2015GL066501) provided important insights on this topic. Therefore, the argument based on Figure S5 is not valid, the images do not clearly show ebullition, and any observed bubbling could be due to other gases, such as oxygen produced by photosynthesis. If the bubbles were indeed methane, the corresponding diffusive fluxes and surface concentration would be extremely high, which is not supported by your data. Please acknowledge that your dataset is biased, as you mentioned, but avoid overinterpreting the results with vague or unsupported statements.

Thank you for this comment. We agree that the methodology used for measuring CH_4 ebullition deserves further clarification, especially given the significance of this flux pathway at TAS3. We have expanded the methodological description in the revised manuscript.

Line 202: Ebullitive fluxes of CO_2 and CH_4 were measured **at the center of the lake** using an inverted funnel submerged below the water surface.

Line 241: Ebullitive fluxes (F_E) of CO_2 and CH_4 were measured in 2023 following the method outlined by Wik et al. (2013). Bubble traps, consisting of inverted funnels with a collection area of 0.23 m^2, were installed for a total 11 days in both lakes (Fig. 2). **The traps were anchored with submerged weights and tied with ropes to fixed shoreline points to minimize movement and drifting. They were positioned near the lake center to improve representativity of ebullition across the central lake area.**

We acknowledge the limitations of using only one bubble trap and the potential for spatial heterogeneity in ebullition rates, as discussed by Wik et al. (2016). However, due to logistical constraints and the small size of the lakes (with diameters of about 10 m), installing multiple traps was not feasible. We now address this limitation in the discussion, emphasizing the need for caution in generalizing ebullitive flux rates from these data and suggesting directions for future work:

Line 605: **However, we acknowledge that our estimates of CH_4 ebullition were based on measurements taken from a single funnel deployed at the center of the lake. This approach restricts the spatial representativeness of the results, especially since ebullition is known to be highly heterogeneous, with localized hotspots often occurring near lake edges or thawing permafrost zones (Wik et al., 2011; Kuhn et al., 2023). This spatial limitation may partially explain the differences observed between the lakes. Future studies should therefore aim to deploy multiple bubble traps across various lake zones to capture this heterogeneity and better constrain whole-lake ebullition estimates.**

We also suggest adding the location of the traps to Figure 1, along with a corresponding note in the caption for clarity:

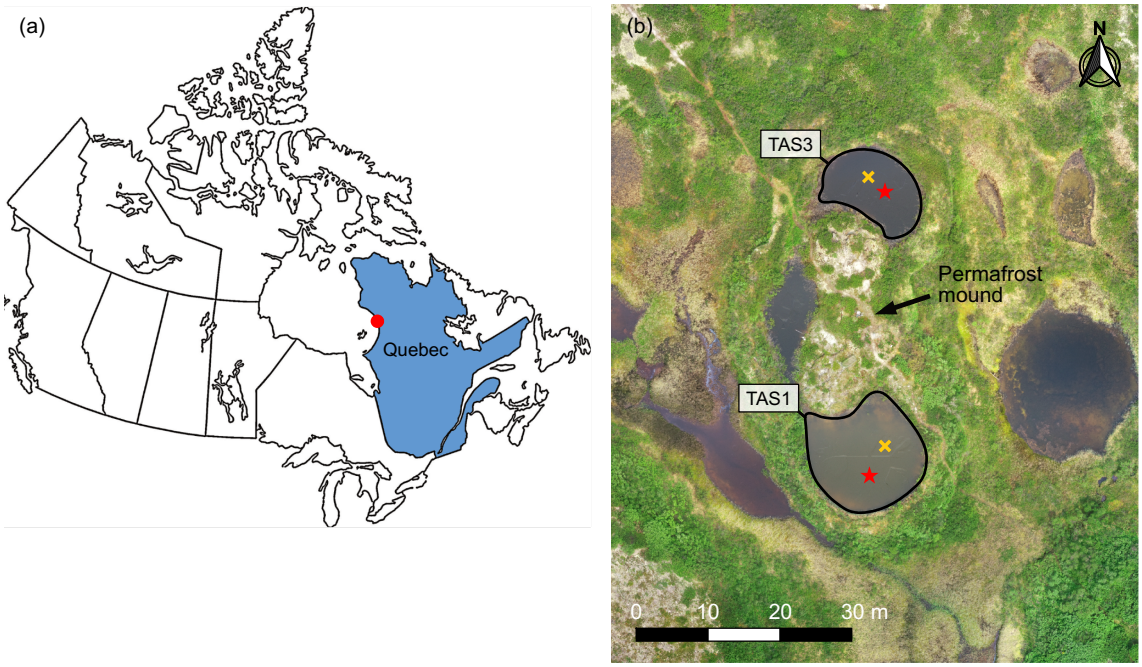

Figure 1. Location map of the Tasiapik Valley: (a) Map of Canada highlighting the study site marked with a red dot, and (b) areal contours of the two lakes under study. **The locations of the mooring lines are marked with red stars, while the bubble traps are marked with yellow crosses.** Aerial photography by Madeleine St-Cyr.

Regarding Figure S5, we agree that the photographs alone are not sufficient to confirm the presence of CH_4. We have removed Figure S5 and the direct reference to visual evidence of bubbling as support for ebullition. To improve transparency, we have now included the exact bubble content data in the dataset available on Borealis. This information has also been specified in the revised manuscript at line 456.

2.4. Regarding the CH_4 and N_2O measurements, I was quite surprised by the reported sensitivity of the GC-TCD, especially its ability to detect concentrations close to atmospheric levels for CH_4 and even lower for N_2O. Are you certain that a TCD was used for these analyses? If so, I strongly recommend that you provide

more detailed information on the calibration procedure, the sample injection volume, and the type of column used. This would be highly valuable for researchers working with similar GC-TCD systems. I am particularly skeptical that N_2O concentrations below atmospheric levels can be reliably detected using a TCD. However, if this is indeed the case, please elaborate on the protocols that enabled such sensitivity.

Thank you for your comment. The GC used for our analyses is equipped with 4 detectors (FID X2, TCD and ECD). We used 2 channels into which 5 mL of gas sample is injected and separated in 2 different injection loops. The first, which is fitted with a TCD and FID detector in series, was used to analyse CH_4 and CO_2. More specifically, the TCD (non-destructive and less sensitive analysis) doses high concentrations, after which the analyte is directed to the FID, which doses lower concentrations. The second, fitted with an ECD detector (which is highly sensitive) analyses nitrous oxide (N_2O) by electron capture. We propose the following clarification in the manuscript:

Line 216: Gas samples were analysed using a Trace 1310 gas chromatograph (Thermo Fisher Scientific). **We used two parallel channels, one with TCD-FID detectors (column HSQ 80/100, MS 5A 80/100) for CH_4 and CO_2, and one with an ECD detector (column HSQ 80/100) for N_2O.** Calibration curves were established for CO_2 (up to 10 000 ppm), CH_4 (up to 45 000 ppm), and N_2O (up to 1 ppm). Detection limits were 200 ppm for CO_2, 3 ppm for low CH_4 concentrations, 50 ppm for CH_4 concentrations above 1000 ppm, and 0.1 ppm for N_2O.

References

Jones, F. E. and Harris, G. L.: ITS-90 density of water formulation for volumetric standards calibration, J. Res. Natl. Inst. Stand. Technol., 97, 335, 1992.

Kuhn, M. A., Schmidt, M., Heffernan, L., Stührenberg, J., Knorr, K.-H., Estop-Aragonés, C., Broder, T., Gonzalez Moguel, R., Douglas, P. M. J., and Olefeldt, D.: High ebullitive, millennial-aged greenhouse gas emissions from thermokarst expansion of peatland lakes in boreal western Canada, Limnol. Oceanogr., 68, 498-513, 10.1002/lno.12288, 2023.

Wik, M., Crill, P. M., Varner, R. K., and Bastviken, D.: Multiyear measurements of ebullitive methane flux from three subarctic lakes, J. Geophys. Res.-Biogeosciences, 118, 1307-1321, 10.1002/jgrg.20103, 2013.

Wik, M., Crill, P. M., Bastviken, D., Danielsson, Å., and Norbäck, E.: Bubbles trapped in arctic lake ice: Potential implications for methane emissions, J. Geophys. Res.-Biogeosciences, 116, G03044, 10.1029/2011JG001761, 2011.

Wik, M., Varner, R. K., Anthony, K. W., MacIntyre, S., and Bastviken, D.: Climate-sensitive northern lakes and ponds are critical components of methane release, Nat. Geosci., 9, 99-106, 10.1038/Ngeo2578, 2016.